BNL-224378-2023-JAAM

Piezoelectric property of PZT nanofibers characterized by resonant piezo-force microscopy

G. Zhang, W. Xu

To be published in "AIP Advances"

March 2022

Photon Sciences

Brookhaven National Laboratory

U.S. Department of Energy

USDOE Office of Science (SC), Basic Energy Sciences (BES) (SC-22)

DISCLAIMER

AIP Advances

Piezoelectric property of PZT nanofibers characterized by resonant piezo-force microscopy

Cite as: AIP Advances **12**, 035203 (2022); https://doi.org/10.1063/5.0081109
Submitted: 16 December 2021 • Accepted: 08 February 2022 • Published Online: 01 March 2022

Guitao Zhang, Xi Chen, Weihe Xu, et al.

Piezoelectric property of PZT nanofibers characterized by resonant piezo-force microscopy

Cite as: AIP Advances 12, 035203 (2022); doi: 10.1063/5.0081109
Submitted: 16 December 2021 • Accepted: 8 February 2022 •
Published Online: 1 March 2022

Guitao Zhang,[1] Xi Chen,[2] Weihe Xu,[3] Wei-Dong Yao,[4] and Yong Shi[1,a)]

AFFILIATIONS

[1] Department of Mechanical Engineering, Stevens Institute of Technology, Hoboken, New Jersey 07307, USA
[2] Advanced Science Research Center (ASRC), Department of Chemical Engineering, The City University of New York, New York, New York 10031, USA
[3] National Synchrotron Light Source II, Brookhaven National Laboratory, Upton, New York 11973, USA
[4] Departments of Psychiatry and Neurosciences, SUNY Upstate Medical University, Syracuse, New York 13210, USA

[a)] **Author to whom correspondence should be addressed:** yshi2@stevens.edu

ABSTRACT

Nano-piezoelectric materials have drawn tremendous research interest. However, characterization of their piezoelectric properties, especially measuring the piezoelectric strain coefficients, remains a challenge. Normally, researchers use an AFM-based method to directly measure nano-materials' piezoelectric strain coefficients. But, the extremely small piezoelectric deformation, the influence from the parasitic electrostatic force, and the environmental noise make the measurement results questionable. In this paper, a resonant piezo-force microscopy method was used to accurately measure the piezoelectric deformation from 1D piezoelectric nanofibers. During the experiment, the AFM tip was brought into contact with the piezoelectric sample and set to work at close to its first resonant frequency. A lock-in amplifier was used to pick up the sample's deformation signal at the testing frequency. By using this technique, the piezoelectric strain constant d_{33} of the Lead Zirconate Titanate (PZT) nanofiber with a diameter of 76 nm was measured. The result showed that d_{33} of this PZT nanofiber was around 387 pm/V. Meanwhile, by tracking the piezoelectric deformation phase image, domain structures inside PZT nanofibers were identified.

In recent years, 1D piezoelectric nanofibers, nanowires, and nanobelts have attracted much research interest. Popular 1D piezoelectric nano-structures, such as ZnO nanowire,[1] ZnO nanoribbon,[2] GaN nanowire,[3] AlN nanowire,[4,5] PZT nanofiber,[6,7] PMN-PT nanowire,[8] $BaTiO_3$ nanowire,[9] Polyvinylidene Fluoride (PVDF) nanofiber,[10–12] and dopped[13,14] or core/shell nanofibers,[15,16] have been fabricated. Material properties, such as Young's modulus, dielectric constant, and piezoelectric voltage constant, have been measured, which all showed difference compared with those of their bulk forms. Various devices based on 1D piezoelectric nano-structures have been proposed and fabricated. Due to their active property that can transform strain energy into electricity, 1D piezoelectric nano-materials become building blocks for nano-generators,[2,16–23] strain sensors,[14,24,25] acoustic sensors,[26] force sensors,[27–29] biosensors,[30] self-powered drug delivery systems,[31] piezoelectric transistors,[32] and other intelligent systems.[20,33]

The most important property of these active materials is their ability to convert mechanical energy into electrical energy and vice versa. This property is described by the piezoelectric constants. The higher the piezoelectric constants are, the more efficient and sensitive a device based on the piezoelectric material will be. On the other hand, since piezoelectric effect is a collective phenomenon, parameters including feature size, grain size, domain wall motion, and substrate constraint all have influence on piezoelectric materials' performance. As a result, researchers started developing nano-sized piezoelectric materials in hope of getting better piezoelectric properties.

To measure the piezoelectric strain constant which represents the materilas's capability to deformation under unit voltage activation, the AFM-based method is widely used. The experimental setup is shown in Fig. 1. In this configuration, an actuation voltage V_{tip} with a DC component (constant voltage V_{dc}) and an AC component

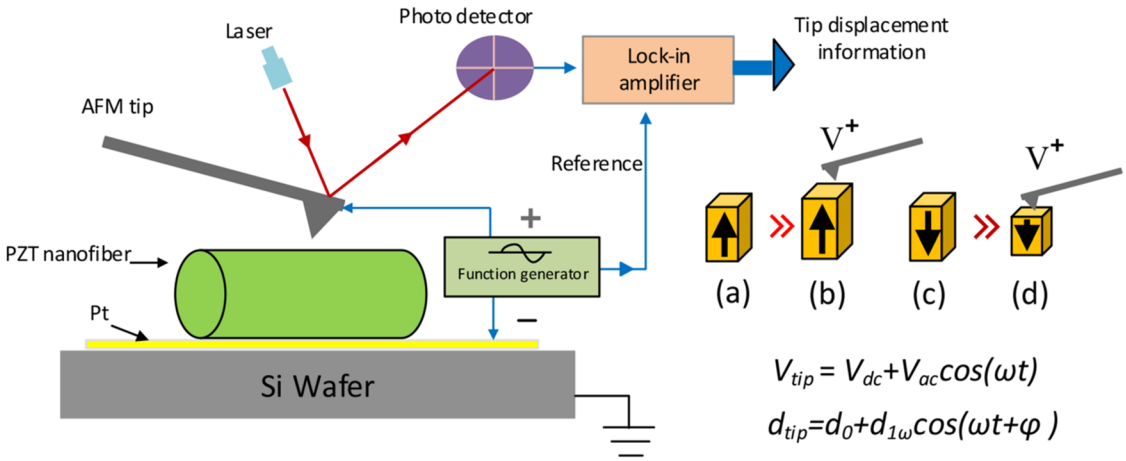

FIG. 1. Piezoelectric strain constant measurement setup. (a) Positive voltage applied to the positively polarized piezoelectric and (b) cause expansion. (c) Positive voltage applied to the negatively polarized piezoelectric and (d) cause contraction.

(alternating voltage V_{ac} with frequency ω) is applied through the AFM tip to the nano-scaled piezoelectric sample. Accordingly, the resulted piezoelectric deformation (d_{tip}) includes a constant deformation part (d_0) and a changing part ($d_{1\omega}$). The DC component V_{dc} is applied to ensure the sample under test will not be depolarized. The AC component is used to trigger a measurable piezoelectric deformation. The piezoelectric deformation will generate a small oscillation voltage on the photodetector with the same vibration frequency ω as the applied AC voltage. By using a lock-in amplifier, the oscillation voltage can be recorded. Then, the voltage can be converted into the sample's deformation amplitude by using the AFM systems' sensitivity number. Furthermore, by measuring the piezoelectric deformation under different voltage amplitudes V_{ac}, an AC voltage and the corresponding piezoelectric displacement relation can be generated. The piezoelectric strain constant d_{33} represents the slope of the voltage–displacement curve.

With this method, some measured nano-scale piezoelectric coefficient data have been reported.[8,34,35] However, there are two major concerns regarding this technique.[36,37] First, the selected testing frequency will have an influence on the results. As a mechanical structure, the AFM tip will output different displacements under AC voltages with the same amplitude but different frequencies, and it may resonant at certain testing frequencies while in contact with the sample. Furthermore, the measurement system or the circuit also has its own frequency response properties. These frequency dependent behaviors may amplify or reduce the true piezoelectric deformation signals. This phenomenon is shown in Fig. 2(a). In this experiment, a PZT nanofiber was tested under different frequencies, ranging from 40 to 80 KHz. The AFM tip's displacement amplitudes and the corresponding activation voltages were plotted together for each testing frequency. The slop of the displacement–voltage curve as shown in the linear fitting equations represents the piezoelectric strain constant d_{33}. We can see that the slop increased from 30.3 to 558.8 pm/V as the testing frequency increased from 45 to 75 KHz. Then, the slop decreases as the testing frequency further increases. Simply using data from one measurement frequency without considering the frequency response property of the testing system is problematic.

A similar testing result was reported by Zhao *et al.*,[35] where they found that the piezoelectric strain coefficient of ZnO nanobelts was frequency dependent and varied from 14.3 to 26.7 pm/V as testing frequencies varied from 15 to 30 KHz, which may be due to the reasons explained above. Second, the electrostatic force between the AFM tip and the substrate will cause errors in the measurement results. The voltage is applied through the conductive AFM tip, while the substrate is grounded; thus, electrostatic force is generated between the AFM cantilever beam, including the AFM tip and the substrate. The electrostatic force will drive the AFM tip to vibrate at the same testing AC frequency. Therefore, the measured AFM tip deformation is the combination of the sample's deformation due to the piezoelectric effect and AFM tip's deformation due to the electrostatic force.

The influence to the measurement result from the electrostatic force is shown in Fig. 2(b). In this experiment, a non-piezoelectric sample SiO_2 film and a well-known piezoelectric sample PMM-PT were measured and compared under a broad testing frequencies with the same activation voltage. The AFM tip's displacement and the corresponding testing frequency were plotted together. As can be seen in Fig. 2(b), the AFM tip on the non-piezoelectric SiO_2 film outputs a non-zero deformation signal, which is totally due to the electrostatic force effect. Moreover, this deformation is also frequency dependent as explained previously. At the frequency of around 70 KHz, the AFM tip started to resonate, which will greatly amplify the measurement results. The deformation from the piezoelectric sample PMN-PT is generally larger than that from the SiO_2 film because it does have an added piezoelectric deformation. As the measurement frequency goes higher, such as above 135 KHz, the output difference between these two samples is much smaller, which is mostly due to the frequency response characteristics of the AFM tip or the photodetector of the AFM system. As a result, we cannot say if a sample has a piezoelectric property purely based on the output signal. For an accurate piezoelectric strain constant

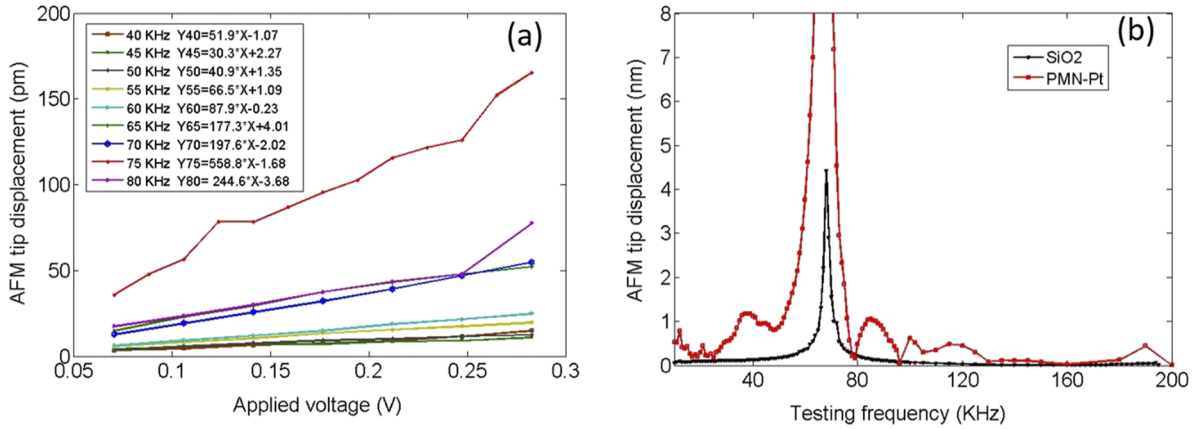

FIG. 2. Influence from the testing frequency and the electrostatic force. (a) Plot of the applied voltage and AFM tip displacement under various test frequencies. (b) PMN-PT and SiO_2 sample deformation measured under different testing frequencies.

measurement, the frequency response characteristics of the system and the electrostatic force influence must be considered.

To address these issues, a resonant piezo-response microscopy method[38] was introduced. In this method, the measurement was performed at the frequency close to the AFM tip's first resonant mode. The frequency response property and the Q factor of the AFM tip as shown in Fig. 2(b) were calibrated with a non-piezoelectric sample. Then, the true sample deformation due to the piezoelectric effect can be obtained by dividing the measurements by the Q factor. Another benefit from working at close to the resonant mode is that the signal-to-noise ratio can be greatly enhanced, which is very important for picking up the extremely small nano-piezoelectric material's deformation signal.

The sample used for this measurement was aligned PZT ($PbZr_{0.52}Ti_{0.48}O_3$) nanofibers on a silicon wafer with a thin layer of silicon dioxide. As was planned to use an AFM-based method for the d_{33} measurement, aligned nanofibers were preferred for the AFM scan process. During the test, a voltage V_{tip} was applied through the AFM tip to the sample, thus effectively preventing short circuit by using a substrate with silicon dioxide. Moreover, silicon dioxide is a non-piezoelectric material, and the response from it can provide a reference to separate the piezoelectric response from the electric static force response. Furthermore, the silicon oxide substrate has an almost perfect flat surface, which is ideal to reduce the topography noise during the AFM scanning process. A SEM image of aligned PZT nanofibers on the silicon dioxide substrate is shown in Fig. 3(a). We can see that the PZT nanofibers are partially aligned with gaps on the order of micro-meters between two adjacent PZT nanofibers. Proper nanofiber density makes it easier to switch between different PZT nanofibers during the AFM scanning process. Figure 3(b) shows partially aligned PZT nanofibers on a platinum substrate. The rough surface from the platinum will introduce much noise in the measurement, and thus, it is not used in this measurement.

The AFM tip used in this test was Arrow-CONTPt, which was a contact AFM probe coated with Pt/Lr. The coating was to make the tip conductive and to enhance the laser reflection from the tip to the

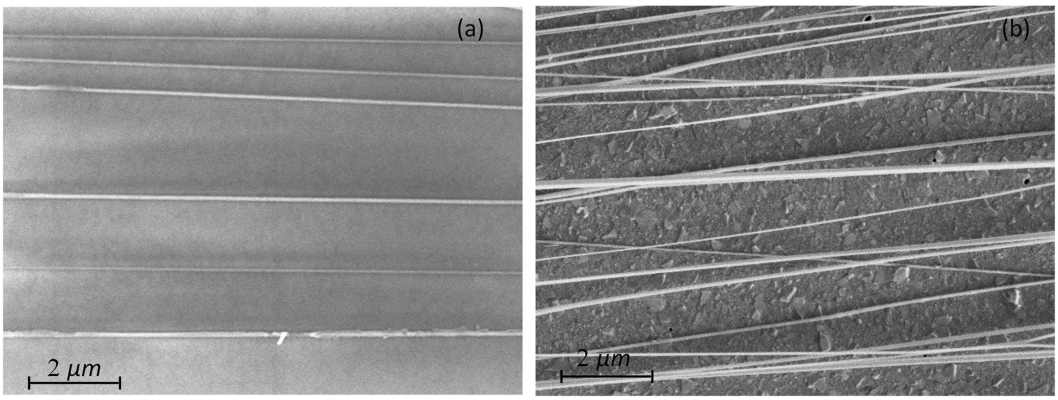

FIG. 3. Partially aligned PZT nanofibers on a SiO2 substrate (a) and on a platinum substrate (b).

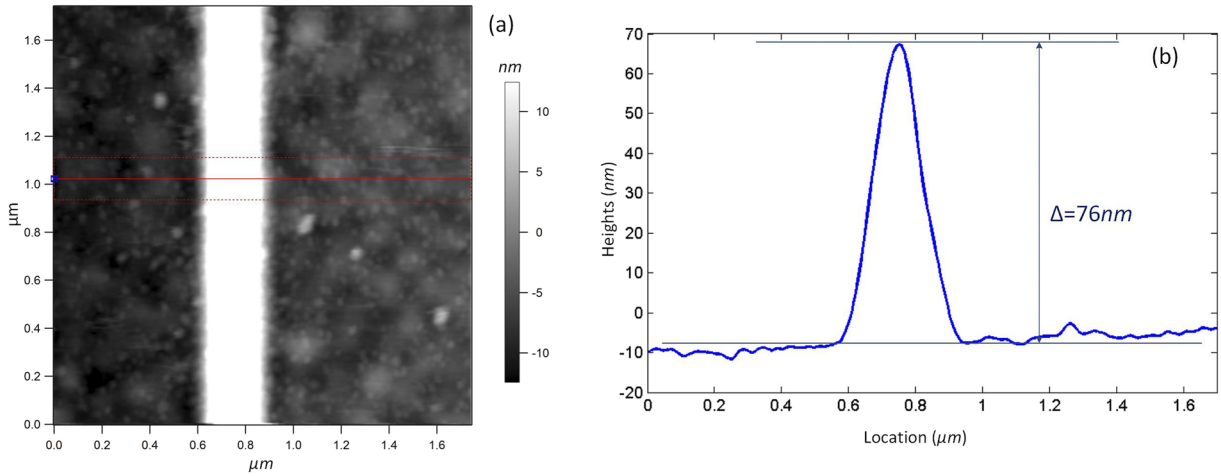

FIG. 4. AFM scan topography image of one PZT nanofiber on the silicon dioxide substrate (a) and its topography profile along the horizontal direction (b).

photodetector. The stiffness of the probe was ~0.2 N/m with a free resonant frequency of ~14 KHz. The stiffness of the probe was low, which can reduce the constrain force applied to the PZT nanofibers. After the AFM tip was brought into contact with the substrate and tuned, the resonant frequency of the AFM trip was increased to ~65 KHz, as the boundary conditions were changed. The measurement frequency was set to be ~60 KHz with an AC voltage of 400 mV, and the DC offset voltage was set at 2.0 V to prevent the sample from depolarizing. The scanned topography image of one PZT nanofiber on a silicon dioxide substrate is shown in Fig. 4(a). An averaged topography profile along the horizontal direction is shown in Fig. 4(b). We can see that the diameter of this PZT nanofiber was 76 nm.

The piezoelectric deformation amplitude image is shown in Fig. 5(a), where we can see a clear contrast between the PZT nanofiber area and the silicon dioxide substrate. The PZT nanofiber had a uniform piezoelectric deformation signal, while the silicon substrate had a much smaller deformation signal, which resulted from thermal noise and electrostatic force. The deformation image contrast between the PZT nanofiber and the silicon dioxide substrate clearly showed the PZT nanofibers' piezoelectric response. A cross-sectional deformation amplitude profile is shown in Fig. 5(b); we can see that the averaged piezoelectric deformation amplitude from the PZT nanofiber was ~155 pm. The thermal noise and the influence from electrostatic force can be identified from the deformation amplitude signal on the silicon dioxide area, which was around 28 pm. Dividing the PZT nanofiber deformation by the activation voltage of 400 mV, the piezoelectric strain constant d_{33} of this PZT nanofiber was calculated to be about 387 pm/V.

The piezoelectric deformation that resulted from the applied AC voltage is a changing item, which not only includes a vibration amplitude component, as shown in Fig. 5(a), but also includes a

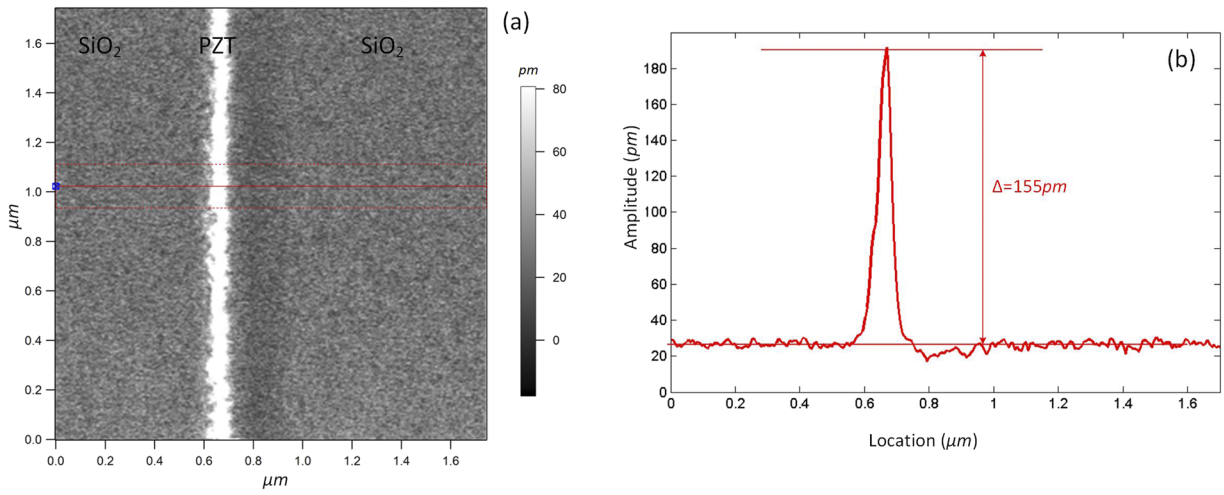

FIG. 5. Piezoelectric deformation amplitude image from a PZT nanofiber on a silicon dioxide substrate (a) and its cross-sectional view along the horizontal direction (b).

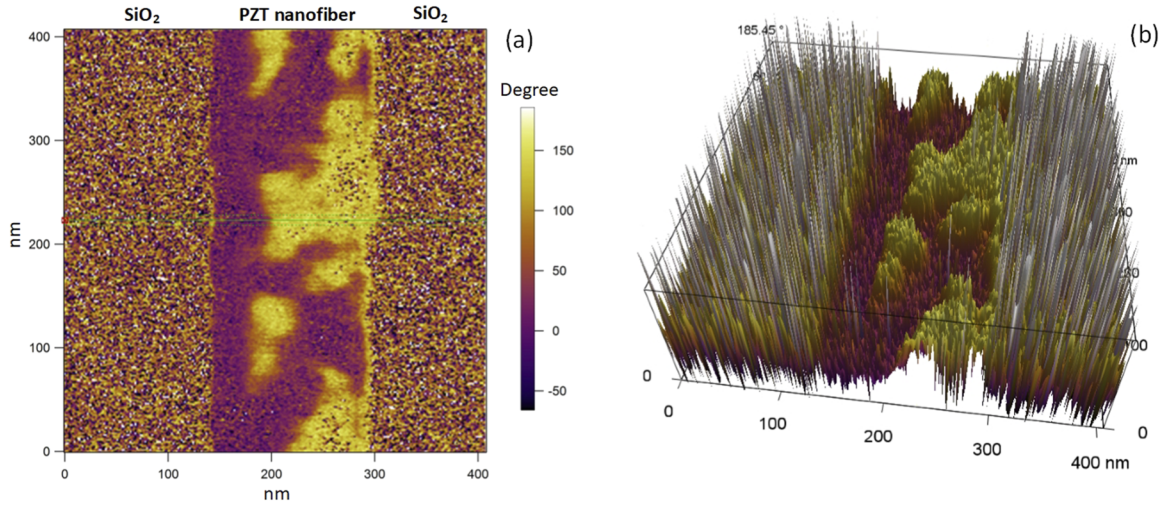

FIG. 6. (a) Piezoelectric deformation phase image from a PZT nanofiber on the silicon dioxide substrate and its 3D image (b).

vibration phase component that can be used to identify the domain structures inside the piezoelectric nanofiber. As shown in Fig. 1(a), assuming that a piezoelectric sample has an initial poling direction upward, it will expand under a positive voltage activation, as shown in Fig. 1(b). For the same activation voltage, a piezoelectric sample with a poling direction downward [Fig. 1(c)] will shrink, as shown in Fig. 1(d). The expansion and shrinkage will be displayed as a vibration phase difference. In the case of two piezoelectric samples whose poling directions are completely opposite, the vibration phase difference will be 180° since their vibration phases are completely opposite to each other, even though they may output the same piezoelectric deformation amplitudes. As a result, the piezoelectric phase images will give information on the domain structure inside a piezoelectric sample. Figure 6(a) shows a piezoelectric deformation phase image from a PZT nanofiber on the silicon dioxide substrate. We can see from Fig. 6(a) that the PZT nanofiber and the substrate had a distinct phase contrast. The PZT nanofiber shows two constant phase groups, which represent two different domains in this PZT nanofiber, while the silicon dioxide substrate shows a rather random phase as yellow and red dots in Fig. 6, which resulted from the random environmental or thermal noise and is expected for a non-piezoelectric material. From the 3D phase image shown in Fig. 6(b), we can see the two domains in the PZT nanofiber more clearly. The phase difference between the two domains is almost 180°, which means that the initial poling directions of these two domains are almost completely opposite.

In this paper, we first discussed the drawbacks of the traditional AFM-based method for piezoelectric material strain constant measurement. The impact from the measurement frequency and electrostatic force was quantified using a piezoelectric material (PMN-PT) and non-piezoelectric material (SiO_2). Then, an improved resonant piezo-force microscopy (PFM) method was used for characterizing PZT nanofibers. In this method, the AFM tip worked at a resonant mode and a silicon dioxide substrate is used to increase the signal-to-noise ratio and to differentiate the sample's deformation signal resulted from the piezoelectric response and from the coupling electrostatic force. The Q factor was pre-calibrated to compensate the influence from the measurement frequency. With this technique, the piezoelectric response from a PZT nanofiber was recorded with picometer accuracy. The PZT nanofibers' piezoelectric strain constant d_{33} was measured to be around 387 pm/V. Furthermore, by using the piezoelectric deformation phase information, domain groups inside a PZT nanofiber were clearly identified. The proposed method will provide a good reference for researchers working on nano-piezoelectric materials.

This research was carried out, in part, at the Center for Functional Nanomaterials, Brookhaven National Laboratory, and is supported by the U.S. Department of Energy, Office of Basic Energy Sciences, under Contract No. DE-AC02-98CH10886.

AUTHOR DECLARATIONS

Conflict of Interest

The authors have no conflicts to disclose.

DATA AVAILABILITY

The data that support the findings of this study are available from the corresponding author upon reasonable request.

REFERENCES

[1] P. Yang, H. Yan, S. Mao, R. Russo, J. Johnson, R. Saykally, N. Morris, J. Pham, R. He, and H.-J. Choi, Adv. Funct. Mater. **12**, 323 (2002).
[2] P.-A. Hu, Y.-Q. Liu, L. Fu, X.-B. Wang, and D.-B. Zhu, Appl. Phys. A **78**, 15 (2004).
[3] X. Duan and C. M. Lieber, J. Am. Chem. Soc. **122**, 188 (2000).
[4] J. Liu, X. Zhang, Y. Zhang, R. He, and J. Zhu, J. Mater. Res. **16**, 3133 (2001).
[5] C. C. Tang, S. S. Fan, M. L. de la Chapelle, and P. Li, Chem. Phys. Lett. **333**, 12 (2001).
[6] S. Xu, Y. Shi, and S. G. Kim, Nanotechnology **17**, 4497 (2006).

[7]G. Zhang, V. Chen, W. Xu, R. Galos, L. Zhou, and Y. Shi, in Proceedings of the ASME Design Engineering Technical Conference, 2014.
[8]S. Xu, G. Poirier, and N. Yao, Nano Lett. **12**, 2238 (2012).
[9]Z. Wang, J. Hu, A. P. Suryavanshi, K. Yum, and M.-F. Yu, Nano Lett. **7**, 2966 (2007).
[10]S.-S. Choi, Y. S. Lee, C. W. Joo, S. G. Lee, J. K. Park, and K.-S. Han, Electrochim. Acta **50**, 339 (2004).
[11]M. Nasir, H. Matsumoto, T. Danno, M. Minagawa, T. Irisawa, M. Shioya, and A. Tanioka, J. Polym. Sci., Part B: Polym. Phys. **44**, 779 (2006).
[12]W. C. Lo, C. C. Chen, and Y. K. Fuh, Adv. Mater. Technol. **6**, 2000779 (2021).
[13]J. Yang, F. Xu, H. Jiang, C. Wang, X. Li, X. Zhang, and G. Zhu, Mater. Chem. Front. **5**, 5679 (2021).
[14]J. Yang, Y. Zhang, Y. Li, Z. Wang, W. Wang, Q. An, and W. Tong, Mater. Today Commun. **26**, 101629 (2021).
[15]S. H. Ji, Y. S. Cho, and J. S. Yun, Nanomaterials **9**, 555 (2019).
[16]J. Han, J. H. Kim, H. J. Choi, S. W. Kim, S. M. Sung, M. S. Kim, B. K. Choi, J. H. Paik, J. S. Lee, and Y. S. Cho, Composites, Part B **223**, 109141 (2021).
[17]X. Chen, S. Xu, N. Yao, and Y. Shi, Nano Lett. **10**, 2133 (2010).
[18]Y. Qi, N. T. Jafferis, K. Lyons, C. M. Lee, H. Ahmad, and M. C. McAlpine, Nano Lett. **10**, 524 (2010).
[19]X. Gao, F. Xing, F. Guo, Y. Yang, Y. Hao, J. Chen, B. Chen, and Z. L. Wang, Mater. Today Energy **22**, 100867 (2021).
[20]H. Askari, N. Xu, B. H. Groenner Barbosa, Y. Huang, L. Chen, A. Khajepour, H. Chen, and Z. L. Wang, "Intelligent systems using triboelectric, piezoelectric, and pyroelectric nanogenerators," Mater. Today (published online, 2022).
[21]Z. Zhu, H. Xiang, Y. Zeng, J. Zhu, X. Cao, N. Wang, and Z. L. Wang, Nano Energy **93**, 106776 (2022).
[22]J. H. Kim, B. Kim, S. W. Kim, H. W. Kang, M. C. Park, D. H. Park, B. K. Ju, and W. K. Choi, Nanotechnology **32**, 145401 (2021).
[23]F. Xu, J. Yang, R. Dong, H. Jiang, C. Wang, W. Liu, Z. Jiang, X. Zhang, and G. Zhu, Adv. Fiber Mater. **3**, 368 (2021).
[24]H. Gullapalli, V. S. M. Vemuru, A. Kumar, A. Botello-Mendez, R. Vajtai, M. Terrones, S. Nagarajaiah, and P. M. Ajayan, Small **6**, 1641 (2010).
[25]J. Zhou, Y. Gu, P. Fei, W. Mai, Y. Gao, R. Yang, G. Bao, and Z. L. Wang, Nano Lett. **8**, 3035 (2008).
[26]X. Chen, J. Li, G. Zhang, and Y. Shi, Adv. Mater. **23**, 3965 (2011).
[27]X. Wang, J. Zhou, J. Song, J. Liu, N. Xu, and Z. L. Wang, Nano Lett. **6**, 2768 (2006).
[28]E. Vorathin, Z. M. Hafizi, N. Ismail, and M. Loman, Opt. Laser Technol. **121**, 10584 (2020).
[29]D. Park and K. Kim, J. Korean Inst. Met. Mater. **59**, 412 (2021).
[30]H. Ouyang, D. Jiang, Y. Fan, Z. L. Wang, and Z. Li, Sci. Bull. **66**, 1709 (2021).
[31]Y. Yang, L. Xu, D. Jiang, B. Z. Chen, R. Luo, Z. Liu, X. Qu, C. Wang, Y. Shan, Y. Cui, H. Zheng, Z. Wang, Z. L. Wang, X. D. Guo, and Z. Li, Adv. Funct. Mater. **31**, 2104092 (2021).
[32]L. Wang and Z. L. Wang, Nano Today **37**, 101108 (2021).
[33]M. S. Sorayani Bafqi, A. H. Sadeghi, M. Latifi, and R. Bagherzadeh, J. Ind. Text. **50**, 1643 (2021).
[34]G. Jikyo, K. Onishi, T. Nishikado, I. Kanno, and K. Kanda, J. Appl. Phys. **130**, 074101 (2021).
[35]M.-H. Zhao, Z.-L. Wang, and S. X. Mao, Nano Lett. **4**, 587 (2004).
[36]S. Kalinin, A. Rar, and S. Jesse, IEEE Trans. Ultrason., Ferroelectr. Freq. Control **53**, 2226 (2006).
[37]S. Jesse, A. P. Baddorf, and S. V. Kalinin, Nanotechnology **17**, 1615 (2006).
[38]R. García, Surf. Sci. Rep. **47**, 197 (2002).